Shear-induced structural transformation and plasticity in ultraincompressible ReB_2 limit its hardness

R. F. Zhang,[1] D. Legut,[2,3] R. Niewa,[4] A. S. Argon,[5] and S. Veprek[1,*]

[1]*Department of Chemistry, Technical University Munich, Lichtenbergstr. 4, D-85747 Garching, Germany*

[2]*Institute of Physics of Materials, Academy of Sciences of the Czech Republic, v.v.i., Žižkova 22, Brno CZ-616 62, Czech Republic*

[3]*Chair of Atomistic Modelling and Design of Materials, University of Leoben, Franz-Josef Strasse 18, A-8700 Leoben, Austria*

[4]*Institute of Inorganic Chemistry, University of Stuttgart, Pfaffenwaldring 55, D-70569 Stuttgart, Germany*

[5]*Department of Mechanical Engineering, Massachusetts Institute of Technology, 77 Massachusetts Avenue, Cambridge, Massachusetts 02139, USA*

(Received 26 June 2010; published 8 September 2010)

The recent search for superhard materials concentrated on diborides of the 5*d* transition metals because of their high elastic moduli. Using density-functional theory we report a systematic study of the shear-induced irreversible structural transformations and plasticity in ReB_2 which limits its strength and hardness. The plasticity is due to breaking and rearrangement of bonds accompanied by crystal-field splitting of 5*d* orbitals from the stabilized to destabilized states during the finite shear that takes place at the atomic level in plastic deformation. Such effects are expected to occur also in diborides of other 5*d* transition metals.

DOI: 10.1103/PhysRevB.82.104104 PACS number(s): 62.20.M−, 62.20.fq, 62.20.de

I. INTRODUCTION

Load-invariant indentation hardness is the average pressure under the indenter during a fully developed plasticity upon large shear whereas zero-pressure elastic moduli describe reversible, infinitesimal elastic deformation close to equilibrium.[1–3] Materials with high bulk modulus attain their high incompressibility through a high valence electron density (VED) of the equilibrium structure,[4,5] whereas achieving superhardness (Vickers hardness of $H_V \geq 40$ GPa) requires also electronic and related structural stability necessary for plastic straining.[4] The experimentally reported proportionality between the indentation hardness and zero-pressure elastic moduli[6,7] is a signature of crystal plasticity because the stress for both the multiplication and mobility of dislocations scales with the shear modulus G_0.[3] However, the proportionality to G_0 does not apply when the material undergoes electronic instability and structural transformation accompanied by softening at finite shear strain prior to or during plastic deformation, since in such cases crystal plasticity occurs at the lower value of plastic shear resistance of that softer structure, not reflecting the original value of G_0.

Much recent search for new intrinsically superhard materials has concentrated on those with high values of elastic moduli.[6–12] Because 5*d* transition metals, such as Os, Re, and W, have large values of bulk moduli, it has been suggested to design superhard materials by incorporating, into these metals, light elements, such as boron, to form strong covalent bonds yet keeping a high VED and bulk moduli.[10–12] A first choice has been OsB_2 because Os possess the highest VED (0.572 electrons/Å^3) and the highest bulk modulus B_0 of 395–462 GPa among transition metals (diamond $B_0 \cong 443$ GPa, e.g., Ref. 4) but low hardness of about 4 GPa because of its nondirectional metallic bonds. However it has been found that the load-invariant hardness of OsB_2 is only ≤ 20 GPa.[13] Using first-principles calculations, Yang *et al.*[14] have shown that, although OsB_2, like other diborides of 5*d* metals, has a high bulk modulus of ≥ 300 GPa, it displays soft behavior within the (001)[010] slip system due to metalliclike shear of the (001) Os-Os layers, formed by Os atoms in adjacent unit cells, because the Os-B bonds are either perpendicular to the [010] direction or are located outside of the Os-Os layer.

Chung *et al.* reported the hardness of ReB_2 of 48 GPa at a relatively low applied load of 0.49 Newton (N) which decreased to about 30 GPa at a load of 4.9 N with a tendency of further decrease at larger load [see Fig. 2A in Ref. 15]. However, as pointed out by Dubrovinskaia *et al.*,[16] the load-invariant hardness of this material is clearly below 30 GPa, i.e., ReB_2 is not superhard. More recently, Levine *et al.*[17] reported a hardness of ReB_2 of only 37.2–40.5 GPa at a low load of 0.49 N and of 28 GPa at a load of 4.9 N. Gu *et al.*[18] have compared the hardnesses of many transition-metal borides and reported hardness of ReB_2 to be about 39.3 GPa at 0.49 N, with a load-invariant hardness of only 26.2 GPa. Otani *et al.*[19] reported hardness of single-crystal ReB_2 of 30.8–35.8 GPa under a load of 1.96 N. Furthermore, these researchers were unable to reproduce the scratching of diamond by ReB_2 as reported by Chung *et al.*[15] (for a possible explanation of the reported scratching of diamond by ReB_2 see Ref. 16). An even lower load-invariant hardness of less than 20 GPa was reported by Qin *et al.*[20] for polycrystalline compacted ReB_2. All these experimental results show that although ReB_2 has a high zero-pressure bulk modulus, i.e., low compressibility, it is not intrinsically superhard.

The crystal structure of ReB_2 may be considered as Re atoms arranged in the motif of a hexagonal closed packing (hcp), although strongly enlarged (about 40%) along [001] direction due to occupation of all tetrahedral voids by B atoms. Short B-B distances occurring within the (001) plane lead to puckered layers of threefold bonded B atoms (similar to those in gray As) with covalent bond distances of about 1.8 Å. Distances B-B along [001] direction are above 3 Å.[21] Recently, Pellicer-Porres *et al.*[22] presented pressure-dependent x-ray absorption spectroscopic data indicating the B layers to flatten on increasing hydrostatic pressures. Dur-

ing this process the pressure-induced reduction in the B-B distances is larger than the reduction in the Re-B distances indicating an increasing B-B covalent bond order. The flattening of the B layers was discussed to reduce the three-dimensional structural rigidity necessary for high hardness.

First-principles calculations have been done in order to determine the elastic and electronic properties of 5*d* transition-metal diborides at equilibrium.[23–26] For example, Chen *et al.*[25] used their high value of the calculated zero-pressure shear modulus G_0 of ReB_2 and Teter's empirical correlation of Vickers hardness with G_0 (Ref. 7) in order to predict the Vickers hardness of ReB_2 to be about 45.2–47.5 GPa, supposedly in agreement with the low-load value of 48 ± 5 GPa reported by Chung *et al.*[15] However as outlined above, this is not the correct value of the load-invariant hardness of ReB_2. We have calculated the stress-strain relationship and have shown that the ideal shear strength of ReB_2 of about 34 GPa is much less than that of c-BN of about 58 GPa, in good agreement with the relative values of the hardnesses of these materials.[27] More recent work has shown that the hardness of TiN, ZrN, and HfN scales with their ideal shear strengths rather than with their shear moduli.[28] Here, we report that the relatively low hardness of ReB_2 is due to shear-induced, irreversible structural transformation into other, softer structures. This provides insight into the atomic and electronic origin of such softening and of the crystal-field instability of the 5*d* orbitals at a large shear that occurs in the regime of fully developed plasticity.

II. COMPUTATIONAL METHODS

Our first-principles calculations of the dependence of total energy and stress on strain were performed using density-functional theory within the generalized gradient approximation (GGA) as implemented in the Vienna *ab initio* simulation package VASP.[29] The electron-ion interaction has been described by projector augmented wave [(PAW)-GGA] scheme. The valence electrons considered were $5d^6$ and $6s^2$ for rhenium and $2s^2 2p^1$ for boron.

We used the unit cell of ReB_2 with two Re and four B atoms in its hexagonal representation. In order to obtain the equilibrium structural parameters, a two-step procedure has been used: first we conducted a full geometry optimization of the cell to obtain a stress-free state, followed by the symmetry analysis. The optimized lattice constants determined in this way were $a_0 = 2.92$ Å and $c_0 = 7.515$ Å, in very good agreement with the published theoretical and experimental values (see Refs. 12, 23, and 27 and references therein). The integration within the Brillouin zone was done using *k* points of $9 \times 9 \times 9$ grids for the crystalline phases under consideration, determined according to the Monkhorst-Pack scheme, energy cutoff of 600 eV, and tetrahedron method with Blöchl corrections for the energy and electronic calculations, and Gaussian smearing for the stress calculations, respectively. We have also verified that the choice of a larger number of the *k* points does not change the results. The conjugate gradient method was used for the relaxation of structural parameters. In order to keep the crystal under a uniaxial stress state, the strained cell has been relaxed for both the atomic basis vectors and for the atom coordinates inside the unit cell by keeping fixed the applied strain component and relaxing the other strain components until their conjugate stress components (i.e., Hellman-Feynman stresses) reached negligible values. To ensure that the strain path is continuous, the starting position at each strain step has been taken from the relaxed coordinates of previous strain step.

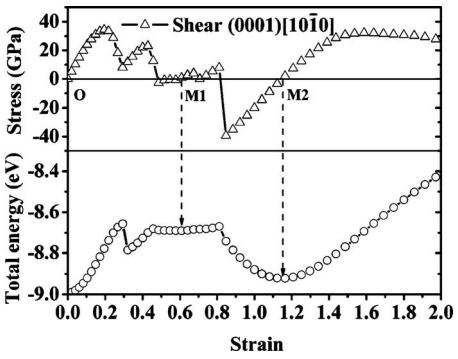

FIG. 1. Dependence of the stress and total energy on the shear strain within the (0001) plane in the [10$\bar{1}$0] direction. The strain points of O, M1, and M2 indicate the equilibrium stable hcp-derived structure and the two metastable trigonal ones formed during the shear-induced phase transformation.

The method of the calculation of the stress-strain dependence has been described and carefully checked in our earlier work.[28,30] For comparison with our VASP calculations, the all-electron full-potential linearized augmented plane-wave method implemented in the WIEN2K code[31] has been used to calculate the orbital-resolved density of states (DOS) of the equilibrium and deformed structures. In these calculations, the same cell as described above for VASP has been used. The results showed reasonable agreement with those obtained from the VASP. Within WIEN2K calculation we used cut-off parameter $R_{MT}K_{max} = 9$, where R_{MT} is the radius of muffin-tin sphere (MT), the maximum value of partial waves inside the MT sphere, $l_{max} = 10$, and the largest reciprocal vector in the charge Fourier expansion $G_{max} = 14$. The number of *k* points in the irreducible part of the Brillouin zone varied from 449 for the hexagonal symmetry of the equilibrium structure O (see below) to 1200 *k* points for the metastable structures of lower symmetry that appear along the stress-strain curve (see below). The total energy was converged to less than 2×10^{-5} Ry/f.u.

III. RESULTS AND DISCUSSION

Figure 1 shows the dependence of the stress and total energy on the shear strain along the weakest (0001)[10$\bar{1}$0] slip system. The units of shear are related to the Re-Re distance within the plane of the sixfold rings so that strain of neighbor Re planes of 1.732 would correspond to full restoration of the original lattice, if it would not collapse earlier. The shear stress increases continuously up to a peak value of about 34 GPa at shear strain of 0.1951, after which it decreases to a local minimum of about 8 GPa at strain of 0.2936. The total energy continuously increases up to a strain

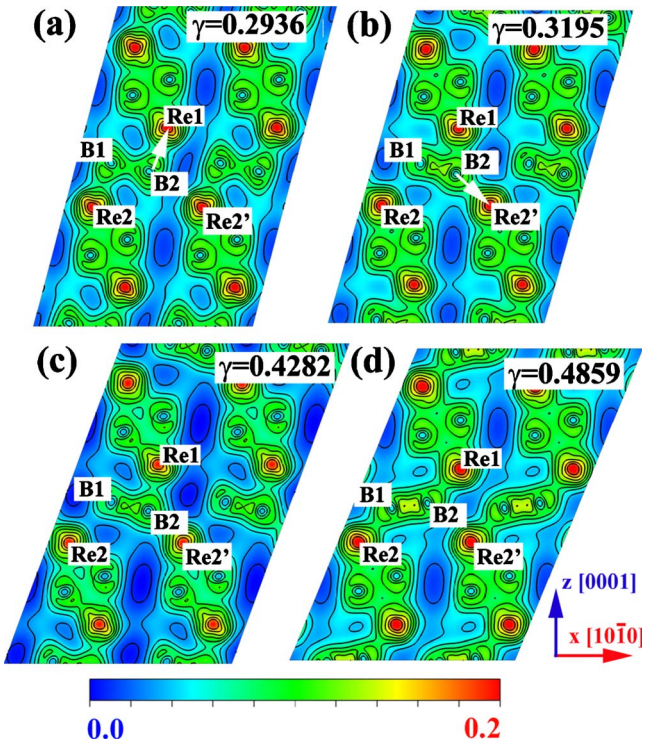

FIG. 2. (Color online) VCD within the (11$\bar{2}$0) plane at the shear strains of (a) γ=0.2936 and (b) γ=0.3195 before and after the first lattice instability, respectively, and (c) γ=0.4282 and (d) γ=0.4859 before and after the second lattice instability, respectively, shown in Fig. 1. Re denotes the rhenium and B the boron atoms. The VCD scale is from 0 (dark blue) to 0.2 (red) in units of electron/bohr^3.

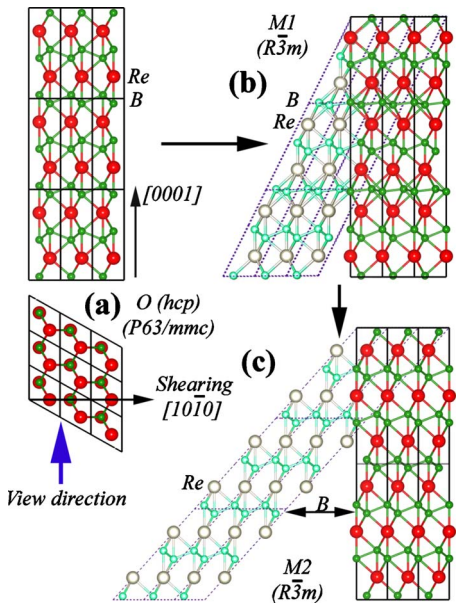

FIG. 3. (Color online) (a) The equilibrium O (hcp) structure from the [11$\bar{2}$0](upper figure) and [0001] crystallographic directions, and the sheared metastable structures of (b) M1 (trigonal) and (c) M2 (trigonal), respectively (see Fig. 1 and the text). Small and large circles represent B and Re atoms, respectively.

of 0.2936 followed by a sharp decrease at shear strain of 0.3195 indicating a lattice instability, which is seen in Figs. 2(a) and 2(b) by the change in valence charge density (VCD) between the strain 0.2936 and 0.3195. During this step the angle of B1-B2 bonds (note that all boron atoms are equivalent; the symbols B1 and B2 are used to identify the given boron atoms in Fig. 2) with respect to the horizontal line rotates clockwise with B1 moving up and B2 down, the bonds B1-Re2 and B2-Re1 almost break and new B2-Re2′ bonds form [see white arrows in Figs. 2(a) and 2(b); note that the symbols Re1, Re2, and Re2′ identify the given rhenium atoms shown in Fig. 2]. Upon further increase in the strain the stress goes through a second local maximum of only about 23 GPa at a strain of 0.4282, followed by its decrease to a value slightly below zero at a strain 0.4859. Simultaneously, the total energy slightly increases reaching a local maximum at a strain of 0.4859 and a very shallow minimum at a strain of 0.6048, which corresponds to a metastable structure denoted M1, because its total energy is higher than that of the initial equilibrium structure O (hcp ReB_2, space group $P6_3/mmc$, number 194, and Pearson symbol $hP6$). As seen in Figs. 2(c) and 2(d), this shear-induced structural transformation occurs at strain of 0.4859 through the anticlockwise rotation of the B1-B2 bond with the B1 atom moving down and the B2 up resulting in the formation of B1-Re2 and B2-Re1 bonds by simultaneously breaking the B2-Re2′ bond, which formed during the first lattice instability at strain of 0.3195. Comparing the calculated VCD before and after lattice instabilities one notices a significant strengthening between B-B bonds during this shear event. The flattened zigzag B-B sixfold rings [Fig. 2(d)] remain preserved during further shear up to a strain of 0.8114 at which the stress is close to zero.

With strain increasing from 0.4859 to about 0.8 (Fig. 1), the stress slightly increases passing zero at strain of 0.6048, where the total energy reaches a very shallow local minimum corresponding to a metastable structure denoted M1 in Fig. 1. Figure 3 shows the transition of the original equilibrium crystal structure [Fig. 3(a)] to the sheared one at point M1 [Fig. 3(b)]. The symmetry analysis[32] of the deformed structure M1 revealed that it is a trigonal structure with the space group $R\bar{3}m$, number 166, and Pearson symbol $hR6$. This structure has been found in some other diborides, such as MoB_2.[33] The lattice parameters in rhombohedral representation are a=7.2511 Å and α=23.7589°. For convenience, this structure in hexagonal representation is shown superimposed on the sheared one in Fig. 3(b) and denoted as M1 (trigonal). With shear strain increasing further above 0.8, another discontinuity is observed in the stress-strain curve (Fig. 1) accompanied by a strong decrease in total energy to a pronounced minimum at a strain of 1.15, where the stress reaches zero, thus showing that a new metastable phase M2 has formed upon that shear event. Using the symmetry analysis of this structure we found [the sheared original and new M2 structure are shown in Fig. 3(c)] that this structure belongs also to the same space group of $R\bar{3}m$ as the M1 (trigonal) structure with lattice parameters in rhombohedral representation being a=4.1257 Å and α=41.463° and Pearson symbol $hR3$. The average atomic volume of the stable structure O is about 9.22 Å^3/atom while that of the M1

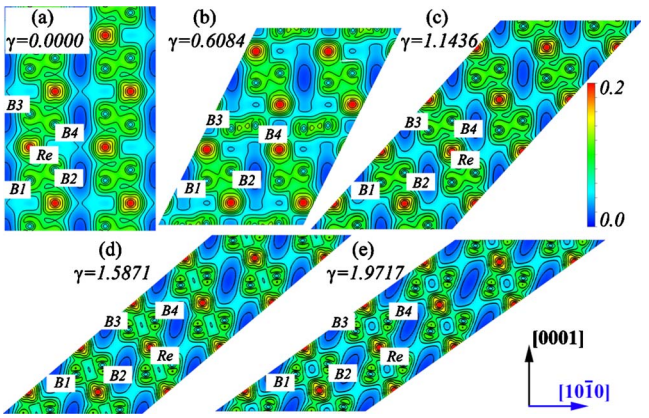

FIG. 4. (Color online) Valence charge density within the (11$\bar{2}$0) plane for several significant values of shear strain γ shown in Fig. 1. Re denotes the rhenium and B the boron atoms. The VCD scale is from 0 (dark blue) to 0.2 (red) in units of electron/bohr^3.

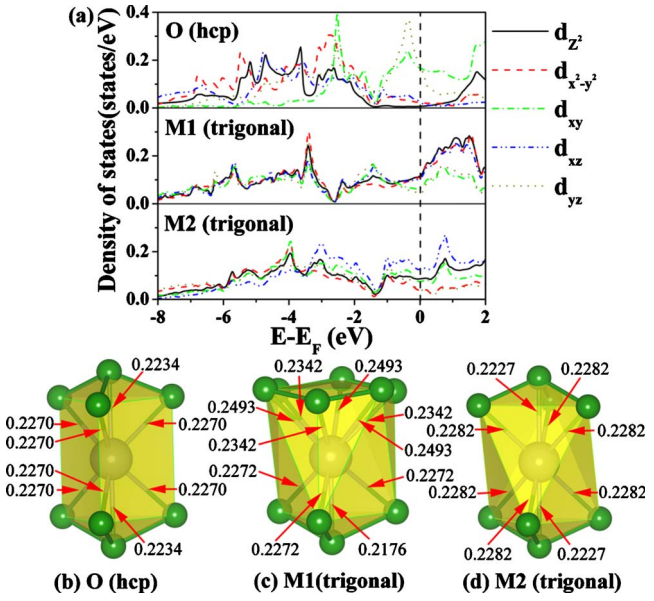

FIG. 5. (Color online) (a) The orbital-resolved density of state of 5*d* levels of rhenium with respect to the Fermi level at equilibrium (O) and of the sheared metastable structures M1 and M2 (see Fig. 1). The axis *x* corresponds to the shear direction [10$\bar{1}$0], *y* axis is parallel to the [11$\bar{2}$0], and *z* to the [0001] direction. Below: the coordination of the rhenium to boron in the three structures (b) O (hcp)-, (c) M1 (trigonal)-, and (d) M2 (trigonal)-ReB$_2$.

structure is 9.06 Å^3/atom and that of M2 of 9.27 Å^3/atom, i.e., the atomic volumes of the metastable structures M1 and M2 are suffering first a compression and then dilatation by −1.76% and +0.5% with respect to the original structure O, characteristic of many stress-induced shear transformations.

The above-mentioned flat zigzag B-B sixfold rings [Fig. 2(d)] persist up to the shear value of 0.8114 after which a large instability on the stress curve is observed, and a second metastable structure M2 is formed. The negative value of the stress between strain of about 0.8114 and 1.1647 together with the relatively deep local minimum of the total energy means that this metastable structure possesses a relatively large stability. This is further illustrated by the increase in the stress up to a maximum value of about 32 GPa at a strain of about 1.6 followed by its small, continuous decrease with strain increasing above 1.6. We recall that a strain of 1.732 corresponds to a full restoration of the original structure O if it had preserved, which is clearly not the case. After just one full shear event, ReB_2 cannot recover even the relatively low ideal shear strength of 34 GPa seen in Fig. 1 at relatively small strain of 0.1951. We recall that this maximum ideal shear strength is much lower than that of c-BN of about 58 GPa.[27] Figure 4 shows that VCD within the (11$\bar{2}$0) plane for several significant values of shear strain γ shown in Fig. 1. It is clearly seen that the shear-induced structural transformation and softening is irreversible because the plasticity by layer sliding between Re-B bonds becomes dominated by lattice dilatation of the B-B bonds (cf. Fig. 4), when the M2 structure is formed after a strain of 0.8114.

The shear-induced softening can also be seen in the changes in the plastic shear resistance by comparing the zero-pressure anisotropic shear modulus G_0 of the original structure of 257.4 GPa (see the first derivative at small strain in Fig. 1) with the first derivatives of the stress-strain curves after the above discussed instabilities, which represent the plastic shear resistance of the given shear-induced, metastable structures. The plastic shear resistance after a first instability at a strain of 0.2936 is reduced to about 149 GPa and decreases further to 58 GPa after the formation of the metastable M1 structure at strain of 0.6048. Upon a further shear, it slightly recovers to about 123 GPa after the formation of the metastable M2 structure but remains much smaller than the G_0 value of 257.4 GPa of the original equilibrium ReB_2 structure (see Fig. 1). One also notices that the shear stress at larger strain never reach the value of 34 GPa, which has been found before the first instability of the original structure O. When the strain increases above about 1.6, the first derivative of the stress with strain becomes negative which means that the structure became inherently instable and collapses. Therefore, it can never return back to the original equilibrium structure O.

A further insight into the electronic origin of the transformations-induced easy plasticity of ReB_2 provide studies of the changes in the orbital-resolved DOS of the 5*d* orbitals of Re atom during the shearing process. Upon shear, the crystal-field splitting and stabilization of energy levels are likely to change as a result of the relative change in the position of the boron atoms with respect to the rhenium ones.[34] Figure 5(a) shows the orbital-resolved DOS of 5*d* orbitals of Re for the three structures with *x* axis along the [10$\bar{1}$0] direction, *y* axis along the [11$\bar{2}$0] direction, and *z* along the [0001] direction. E_F corresponds to the Fermi level. The dominant contribution to DOS at the Fermi level comes from two 5*d* orbitals of d_{yz} and d_{xy} for the O (hcp) structure, three orbitals of d_{z2}, d_{x2-y2}, and d_{xz} orbital for the M1 (trigonal) structure, and three orbitals of d_{z2}, d_{xz}, and d_{xy} for the M2 (trigonal) structure. The changes in the resolved 5*d* orbitals at the Fermi level are summarized as follows

(notice that one and two vertical arrows mean medium and large effect, respectively):

$$\mathrm{O\ (hcp)} \rightarrow \mathrm{M1\ \ (trigonal)} \rightarrow \mathrm{M2\ \ (trigonal)},$$

$$d_{z^2} \quad 0.0065 \rightarrow 0.1166(\uparrow\uparrow) \rightarrow 0.0858(\downarrow),$$

$$d_{x^2-y^2} \quad 0.0225 \rightarrow 0.1103(\uparrow\uparrow) \rightarrow 0.0377(\downarrow\downarrow),$$

$$d_{xy} \quad 0.1675 \rightarrow 0.0640(\downarrow\downarrow) \rightarrow 0.0740(\uparrow),$$

$$d_{xz} \quad 0.0250 \rightarrow 0.1042(\uparrow\uparrow) \rightarrow 0.1264(\uparrow),$$

$$d_{yz} \quad 0.1733 \rightarrow 0.0450(\downarrow\downarrow) \rightarrow 0.0386(\downarrow).$$

It can be seen that upon the transformation from the stable O (hcp) to the metastable M1 structure during the $(0001)[10\bar{1}0]$ (xz) shear, the d_{xy} and d_{xz} states at Fermi level are stabilized whereas d_{z^2}, $d_{x^2-y^2}$, and d_{xz} are strongly destabilized, which explains the large instability of the M1 structure. The transformation of M1 to M2 is accompanied by opposite changes in the d orbitals at Fermi level but it does not bring them quite back to the values of the original O (hcp) structure. This analysis provides a qualitative explanation why the M2 (trigonal) phase is more stable than the M1 (trigonal) one, both being metastable with respect to the equilibrium O (hcp) structure (Fig. 1). The relative stabilization of the three phases can also be seen from the change in coordination of rhenium surrounded by boron atoms during the phase transition as shown in Figs. 5(b)–5(d). Upon the transition from O to M1, the zigzag B-B sixfold ring flattens and the layer slips until Re comes at a place directly below the sixfold B ring as shown in Fig. 6. Upon a further increase in the strain the layer slips along the same vector until, in the M2 structure, the Re has a similar coordination as in O, however the orientation of the boron "triangle" above is rotated by 60° relative to the bottom triangle.

As mentioned above, for a strain larger than about 1.6, the stress decreases with increasing strain showing that the structure became inherently instable. In order to understand the electronic origin of this instability we show in Fig. 7 the line profiles of the VCD between the B-B and Re-B bonds in equilibrium, for shear strain of 1.1436 that corresponds to the last maximum of stress, and for strain of 1.5871 and 1.9717 where the shear stress decreases with increasing strain (see Figs. 1 and 4). One can see that there is no noticeable difference in the lines in equilibrium and at strain of 1.1436 [see Figs. 7(a) and 7(b)] and the B-B bonds are significantly stronger than the Re-B ones [cf. Figs. 7(c) and 7(d)]. This means that the covalently bonded B rings are the main carrier of the load, holding the ReB_2 structure together, whereas the contribution of the Re-B bonds is relatively small. For larger shear strain, where the shear stress decreases with increasing strain displaying an inherent instability of the structure, the B-B bonds break, whereas little change is seen in the weak Re-B ones. This is the reason of the irreversible electronic and concomitant structural transformations which result in a collapse of the structure.

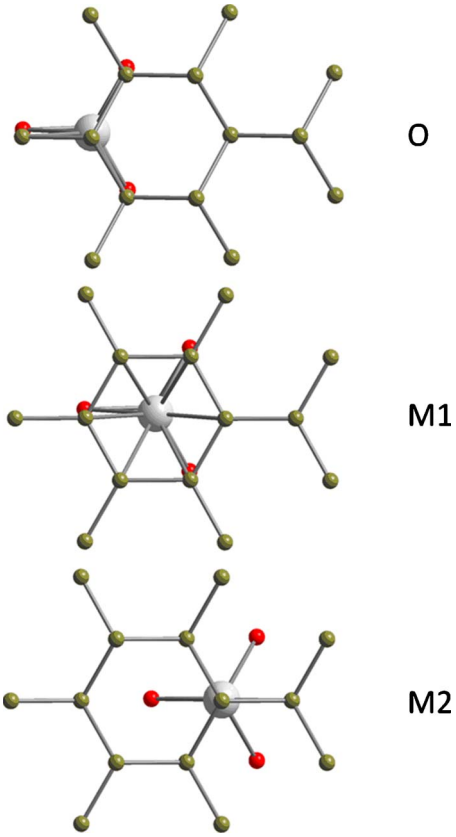

FIG. 6. (Color online) Top view of the changes in the coordination of Re in the three structures (a) the equilibrium O (hcp)-, and the metastable (b) M1 (trigonal)- and (c) M2 (trigonal)-ReB_2 during the shear. With the Re and the 3 B (in red) as the unaffected layer below, the brownish B-"zigzag hexagon" layer moves from right to left in the figures on going from O to M1 and M2. During this process, the zigzag B-B sixfold ring flattens (M1) and the layer slips until Re comes at place directly below the sixfold B ring. In this case, the flattened B layer can be interpreted as close to a graphitic (not completely flat), i.e., B with double-bond contributions reducing the bond length (however, the bond reduction is certainly also necessary to fit the geometric extension of the unaffected layer). On further increase in strain the layer slips along the same vector until Re resides in M2 in a similar coordination as in O. However the orientation of the boron triangle above Re is turned by 60° relative to the bottom triangle.

IV. CONCLUSIONS

In conclusion, we have shown that shear-induced structural transformation in ReB_2 results in low plastic shear resistance (softening) of the new metastable phases which do not recover even upon a full shear step because of irreversible changes and collapse of the electronic structure. The shear-induced instability of the equilibrium O structure that occurs at a relatively small shear strain of 0.1951 is closely related to the relatively strong B-B bond within that structure, and it limits the plastic shear resistance of ReB_2. Upon a further shear, metastable trigonal structures with a reduced plastic shear resistance are formed but the original, equilibrium structure is not recovered even after a full shear step of the shearing planes signifying a permanent structural trans-

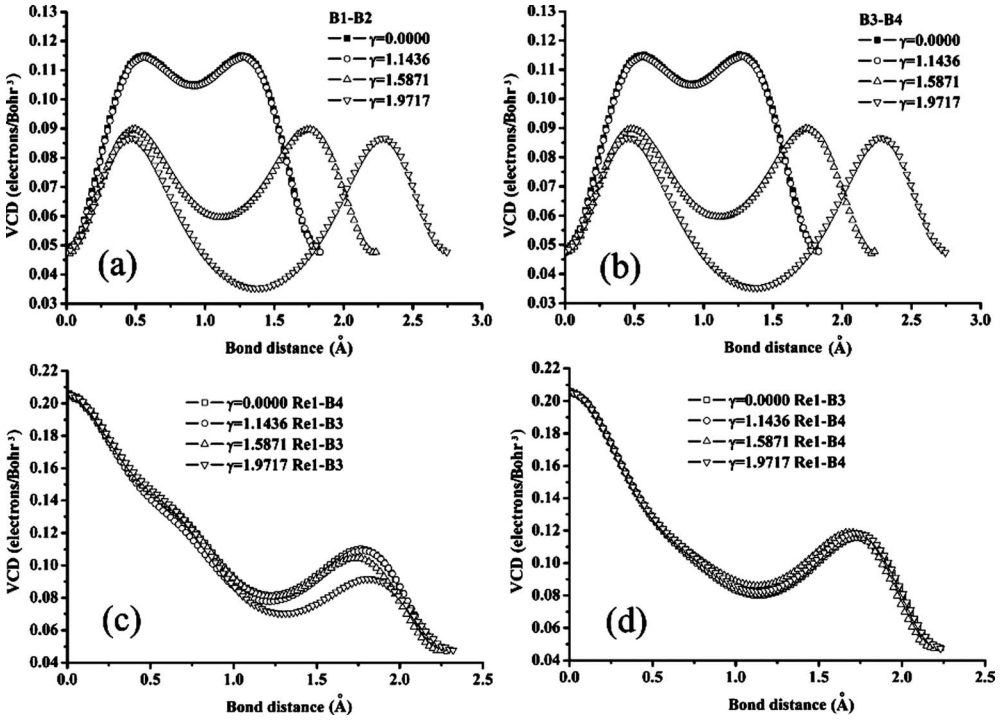

FIG. 7. Line profiles of the VCD between the B-B and Re-B bonds in equilibrium and for several significant values of shear strain γ shown in Figs. 1 and 4.

formation. This behavior is closely related to the electronic 5*d* structure which shows complex changes and destabilization due to the crystal-field splitting upon the shear. In the final stage of the shear-induced instability, the B-B bonds, which provided the material with its strength at the smaller shear, break and the whole system collapses. These effects will probably limit the achievable hardness of other diborides of 5*d* transition metals in spite of their high elastic moduli.

ACKNOWLEDGMENTS

This work has been supported by the German Research Foundation (DFG) and by the European Commission within the project NoE EXCELL under Contract No. 5157032. The research of A.S.A. at MIT was supported by the Mechanical Engineering Department. D.L. was partially supported by Research Project No. AV0Z20410507 by Czech Science Foundation.

*Corresponding author. FAX: +49 89 28913626; stan.veprek@lrz.tum.de

[1] G. Tabor, *The Hardness of Metals* (Clarendon Press, Oxford, 1951).
[2] S. Vepřek, J. Vac. Sci. Technol. A **17**, 2401 (1999).
[3] A. S. Argon, *Strengthening Mechanisms in Crystal Plasticity* (Oxford University Press, Oxford, 2008).
[4] Y. Zhang, H. Sun, and C. F. Chen, Phys. Rev. B **73**, 064109 (2006).
[5] R. F. Zhang, S. Veprek, and A. S. Argon, Phys. Rev. B **80**, 233401 (2009).
[6] J. Haines, J. M. Leger, M. Schmidt, J. P. Petitet, A. S. Pereira, and J. A. H. da Jordana, in *High Pressure Research in Biosciences and Biotechnology*, edited by K. Heremans (Lwuven University Press, Leuven, 1997).
[7] D. M. Teter, MRS Bull. **23**, 22 (1998).
[8] M. L. Cohen, Phys. Rev. B **32**, 7988 (1985); Solid State Commun. **92**, 45 (1994).
[9] A. Y. Liu and M. L. Cohen, Science **245**, 841 (1989).
[10] J. B. Levine, S. H. Tolbert, and R. B. Kaner, Adv. Funct. Mater. **19**, 3519 (2009).
[11] J. B. Levine, J. B. Betts, J. D. Garrett, S. Q. Guo, J. T. Eng, A. Migliori, and R. B. Kaner, Acta Mater. **58**, 1530 (2010).
[12] R. B. Kaner, J. J. Gilman, and S. H. Tolbert, Science **308**, 1268 (2005).
[13] H. Y. Chung, J. M. Yang, S. H. Tolbert, and R. B. Kaner, J. Mater. Res. **23**, 1797 (2008).
[14] J. Yang, H. Sun, and C. F. Chen, J. Am. Chem. Soc. **130**, 7200 (2008).
[15] H. Y. Chung, M. B. Weinberger, J. B. Levine, A. Kavner, J. M. Yang, S. H. Tolbert, and R. B. Kaner, Science **316**, 436 (2007).
[16] N. Dubrovinskaia, L. Dubrovinsky, and V. L. Solozhenko, Science **318**, 1550 (2007).
[17] J. B. Levine, S. L. Nguyen, H. I. Rasool, J. A. Wright, S. E. Brown, and R. B. Kaner, J. Am. Chem. Soc. **130**, 16953 (2008).
[18] Q. Gu, G. Krauss, and W. Steurer, Adv. Mater. **20**, 3620 (2008).

[19] S. Otani, M. M. Korsukova, and T. Aizawa, J. Alloys Compd. **477**, L28 (2009).
[20] J. Q. Qin, D. W. He, J. H. Wang, L. M. Fang, L. Lei, Y. J. Li, J. Hu, Z. L. Kou, and Y. Bi, Adv. Mater. **20**, 4780 (2008).
[21] O. J. Żogał, Z. Fojud, P. Herzig, A. Pietraszko, A. B. Lyashchenko, S. Jurga, and V. N. Paderno, J. Appl. Phys. **106**, 033514 (2009).
[22] J. Pellicer-Porres, A. Segura, A. Munoz, A. Polian, and A. Congeduti, J. Phys.: Condens. Matter **22**, 045701 (2010).
[23] X. Hao, Y. Xu, Z. Wu, D. Zhou, X. Liu, X. Cao, and J. Meng, Phys. Rev. B **74**, 224112 (2006).
[24] W. Zhou, H. Wu, and T. Yildirim, Phys. Rev. B **76**, 184113 (2007).
[25] X. Q. Chen, C. L. Fu, M. Krcmar, and G. S. Painter, Phys. Rev. Lett. **100**, 196403 (2008).
[26] X. L. Zhu, D. H. Li, and X. L. Cheng, Solid State Commun. **147**, 301 (2008).
[27] R. F. Zhang, S. Veprek, and A. S. Argon, Appl. Phys. Lett. **91**, 201914 (2007).
[28] R. F. Zhang, S. H. Sheng, and S. Veprek, Appl. Phys. Lett. **94**, 121903 (2009).
[29] G. Kresse and J. Furthmüller, Comput. Mater. Sci. **6**, 15 (1996).
[30] R. F. Zhang, S. H. Sheng, and S. Veprek, Appl. Phys. Lett. **90**, 191903 (2007); **91**, 031906 (2007).
[31] K. Schwarz and P. Blaha, Comput. Mater. Sci. **28**, 259 (2003).
[32] R. F. Zhang and S. Veprek, Acta Mater. **57**, 2259 (2009).
[33] S. Okada, T. Atoda, I. Higashi, and Y. Takahashi, J. Mater. Sci. **22**, 2993 (1987); M. Frotscher, W. Klein, J. Bauer, C. M. Fang, J. F. Halet, A. Senyshyn, C. Baehtz, and B. Albert, Z. Anorg. Allg. Chem. **633**, 2626 (2007).
[34] A. F. Cotton and G. Wilkinson, *Advanced Inorganic Chemistry*, 3rd ed. (Wiley, New York, 1972), pp. 556–561.